arXiv:1211.0422v1 [math.GT] 2 Nov 2012

A state sum invariant of tangles on surfaces *

Peter M. Johnson Sóstenes Lins

November 5, 2012

Abstract

In this paper we define a new state sum based on the regions defined by tangles on a surface which is an oriented closed surface with a finite number of open holes drilled. From this state sum we obtain an invariant of regular isotopy for the tangles named u-invariant. The values of the u-invariant are in $\mathbb{Z}[u]$, where u is a primitive fifth root of the unity. Various basic properties of the invariant are proved and discussed. It can be specialized to invariants of framed links in $\mathbb{R}^3$. Its categoric aspect is emphasized: composition of tangles in surfaces correspond to matrix multiplication. The values of the u-invariant conjugate under taking the mirror of the tangle.

1 Introduction

This work has its inspiration in the 3-manifold invariants introduced the seminal papers of Turaev and Viro [8] which assign a symbol in an alphabet $\{0, \ldots, r-1\}$ to the 2-cells of a special spine of a 3-manifold and on the paper by Reshetikhin and Turaev [6] which assign one of these symbols to the faces and components of a projection on S^2 of a link in S^3 representing a 3-manifold by surgery instructions. See also Lickorish [5] and Kauffman-Lins [4] for connections of the Reshetikhin-Turaev theory with the Temperley-Lieb Algebra and the Jones polynomial.

Our motivating idea was trying to generalize the invariant of Witten-Reshetikhin-Turaev (WRT) by proceeding from a defined state sum in complete general algebraic terms obtaining equations from the moves in such a way that once a Groebner Basis for the associated ideal is obtained an ideal invariant is defined for the tangles. In many cases we go beyond the Groebner basis by decomposing the ideal into primary ideals. This is how we singled out the u-invariant, which is the simplest possible having $r = 2$.

As a particular case, the u-invariant applies to framed links on surfaces. Important facts about the u-invariant are: (a) it is very simple to define, (b) has substantially fewer states than the Jones polynomial (c) requires almost no machinery to prove its invariance and (d) it is fairly strong. Moreover u has some nice structural properties which curtail the complexity of its computation.

In more concrete terms, the value of the u-invariant in a tangle T is a polynomial $a\,u + b\,u^2 + c\,u^3 + d\,u^4$, where a, b, c, d are integers and u is a fixed primitive fifth root of 1. Taking mirror images of the tangles correspond to conjugate the respective u-invariant polynomials, fact that motivates the normalization which removes the term independent of u by using $1 + u + u^2 + u^3 + u^4 = 0$.

The u-invariant is the simplest case (we can say that it is a toy case) of a general family of invariants of tangles, links and 3-manifolds based on the notion of *well-conected tangles*, defined and treated in a companion paper [3] by the same authors.

The paper is organized as follows. In Section 2 we define well-conected tangles and their bracket facial expansions. Section 3 proves the invariance of u. Section 4 and 5 are appendices showing respectively the values of the u-invariant based on the 249 prime knots up to 10 crossings.

We are indebted to the Departamento de Matemática, UFPE, Brazil and to the Centro de Informática, UFPE, Brazil for finantial support. The second author is also supported by a research grant from CNPq/Brazil, proc. 301233/2009-8.

2 The basic object: the (p, m, n)-tangle

Let S be a compact oriented surface of genus p with k boundary components. We can think of S as a sphere with a p orientable handles attached from which $k = m + n$ disjoint open disks are removed. We consider these holes ordered. A *tangle* on a surface S is a finite number of curves crossing transversally, each one either closed or with endpoints on the boundary ∂S. Each hole has a cyclically ordered set of endpoints of the tangle. At a crossing

---

[*] 2010 Mathematics Subject Classification: 57M27 (primary), 57M25 (secondary)

of T the distinction between the underpass and the overpass is given. By a tangle T we always mean a tangle on a surface S. A face of a tangle is a connected component of $S \backslash T$. The first m holes form the *upper boundary* of the tangle and the last n holes form the *lower boundary* of it. The *type* of S is (p, m, n) and T is named a (p, m, n)-tangle, see Fig. 1. In order to produce evaluations which lead to invariants under Reidemeister moves we use the definition of well-connected tangle introduced in [3].

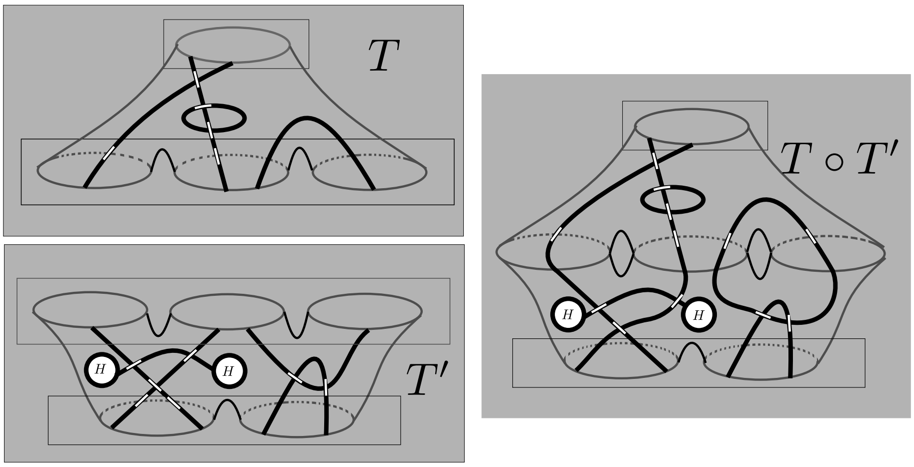

Figure 1: Composition of tangles on surfaces: if T is a (p, m, n)-tangle and T' is a $q, n, r)$-tangle, then the composite tangle $T \circ T'$ can be defined in the natural way, so that the order of the n holes to be matched as well as the cyclic ordering of the endpoints of the tangles agree. Here, specifically, the tangle T which is a $(0, 1, 3)$-tangle is composed with T' which is a $(1, 3, 2)$-tangle. One handle is defined by removing the disks labeled H and identifying the holes, so that $q = 1$. The result of the composition is the $(1, 1, 2)$-tangle $T \circ T'$.

(2.1) Definition. A tangle T is *well-connected* if each face f is an open disk or a cylinder whose boundary ∂f in S intersects ∂S in a connected set, which in the second case is a boundary component of S free of endpoints.

3 A facial state sum evaluation of $(p, m, n, \Upsilon, \Lambda)$-tangles

From now on tangles are well-connected. The evaluation of tangles that follows leads to the simplest example of an invariant for tangles under Reidemeister moves (the *u-invariant*) based on the theory introduced in the foundational article [3]. The u-invariant is, in a sense, a toy invariant of the theory because many enhancements are possible. Our main objective is to obtain a fairly strong invariant based on a facial state sum on a tangle which has substantially less states than 2^n, where n is the number of crossings.

We define a *state of a well-connected tangle* to be a function which puts either a white dot or a black dot inside the disks associated to the faces, provided two faces receiving a black dot do not share an edge. Under such a function, we can distinguish 5 variables that can be associated with a crossing, induced by the state. To obtain the variable, we rotate the crossing such that the overpass is from northeast to southwest. Next we read the dots anticlockwise starting from the east. A 4-bit binary number (a $4j$) is formed this way (a white dot is 0, a black dot is 1). The variables $\{z, a, b, e, j\}$ are defined as in Fig. 2. Note that under a π-rotation, $a = d$ and $b = h$.

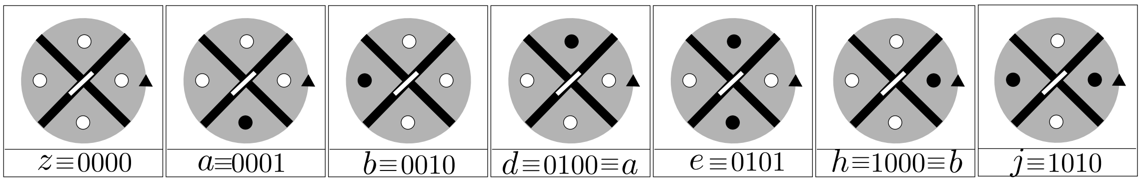
z≡0000 a≡0001 b≡0010 d≡0100≡a e≡0101 h≡1000≡b j≡1010

Figure 2: Scheme to associate variables to the crossings induced by the states

In addition to these 5 variables related to crossing we use two more: x and y, which are related to faces. The monomial ξ_σ is the product of the variables induced by σ in the crossings.

The faces of a tangle is either an *internal face* (when it meets the boundary of no hole) or a *boundary face* (when it meets the boundary of one hole). Note that by definition of well-connectedness, a face meets at most one hole. Let υ and λ be partial states restricted respectively to the faces that meet the upper boundary and to the faces that meet the lower boundary. No face can meet both the upper boundary and the lower boundary. Let Υ and Λ, denote the set of possible values for respectively υ and λ. The role of Υ and Λ in the evaluation of tangles is so proeminent that it is convenient to incorporate them in the notation for the type of the tangle. The *evaluation of a* $(p, m, n, \Upsilon, \Lambda)$*-tangle* T is the $(\Upsilon \times \Lambda)$-matrix $[T]$ whose (υ, λ)-entry is the sum

$$\sum_{\sigma} \left\{ x^{w(\sigma)} y^{b(\sigma)} \sqrt{x}^{w'(\sigma)} \sqrt{y}^{b'(\sigma)} \xi_\sigma \mid \sigma \text{ extends } \upsilon \text{ and } \lambda \text{ to the internal faces} \right\} \in \mathbb{Z}[z, a, b, e, j, \sqrt{x}, \sqrt{y}] = \mathcal{R}\surd,$$

where $w(\sigma)$ and $b(\sigma)$ are, respectively, the number of white dots and black dots in the image of σ in the internal faces. Similarly for $w'(\sigma)$ and $b'(\sigma)$ but in the boundary faces instead. Observe that Υ, Λ or both can be empty. This evaluation is tailored to make true the following theorem:

(3.1) Theorem. *Suppose that* T *is a* $(p, m, n, \Upsilon, \Lambda)$*-tangle and* T' *is a* $(q, n, r, \Lambda, \Gamma)$*-tangle. Then, the evaluation of the* $(p + q, m, r, \Upsilon, \Gamma)$*-tangle* $T \circ T'$ *is the matricial product of the evaluation of* T *and the evaluation of* T'*, namely,*

$$[T \circ T'] = [T]\,[T'].$$

Proof. Straightforward from the definitions. □

In the case that Υ and Γ are empty, tangle $T \circ T'$ is on a surface without holes and there are no tangle endpoints. In this case no square roots appear and $[T \circ T'] \in \mathbb{Z}[z, a, b, e, j, x, y] := \mathcal{R} \subset \mathcal{R}\surd$. The order of the resulting matrix in this case is 1×1.

3.1 Forcing invariance under the restricted Reidemeister move 2

Henceforth a tangle means a $(p, m, n, \Upsilon, \Lambda)$-tangle in a surface which is well-connected. For our purposes Reidemeister move 2 is only applicable when the two faces f and g which are opposite to the region bounded by the digon in its vertices are distinct, refer to Fig. 3. If it is the case globally that $f \neq g$, then the move depicted in this figure is *admissible* and can be performed.

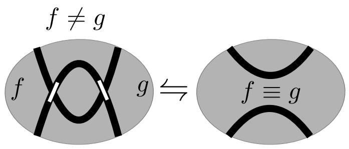

Figure 3: Non-locallity of Reidemeister move 2

In a general context we can replace the admissible (non-local) move 2 by factoring it via the four local moves of Fig. 4, as proved in [3].

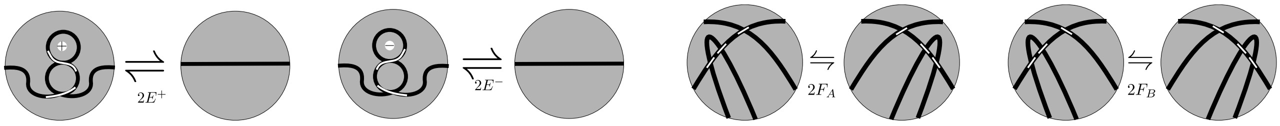

Figure 4: **Moves that factor an admissible move 2**

While the factorization is handy for general graphical calculus, here we can deal directly with the non-local move 2 knowing that it is admissible. Since this is a lot shorter than considering the 4 local moves of Fig. 4, it is the road we take.

In Fig. 5 we consider all the possible boundary restricted states around the neighborhood of an admissible non-local move 2. Of the 16 assignments for the boundary faces 9 have 1-1 adjacency and are automatically ruled out. Each left side of an equation is a sum of at most two monomials. Each right side is a monomial. The boundary color configurations where two monomial are present are 0,2,8 and 10. In these cases the internal digon has a spot which is half white half black, to indicate a superposition of two colors. The resulting states induce, respectively, a variable with white background and a variable with black blackground. The product of the white background variables defines one monomial and the product of the black background variables defines the other monomial. Since we are under admissible 2-moves, for each one of the seven state remaining three **distinct** faces at the left coalesce into a single face at the right. We need this count to adjust the exponents of x and y. In cases labelled 2 and 8, the right diagrams are incompatible as the same face receives a white and a black spot, and so, must be evaluated as 0. It follows that the polynomials can explicitly written, no ambiguity is present. Cases 1 and 4 induce the same polynomial and so, six polynomials are sufficient to induce invariance. More explanation in the caption of Fig. 5.

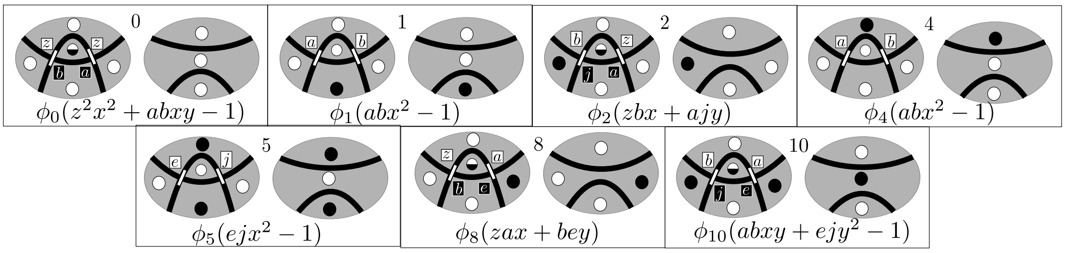

Figure 5: Six polynomials inducing invariance of tangle evaluation under an admissible non-local Reidemeister 2-move. A problem with this non-local move is that the boundaries before and after the move do not coincide. Thus we have to think on the above diagrams as fragments of a global well-connected tangle. The monomial factors ϕ_i take care of any complete state which extends the states restricted to the fragments. By well-connectedness at least one of the leftmost and rightmost face is an internal face. So, square root occurrences can be absorbed by the monomial factor ϕ_i and we are left with six pairs of polynomials in $\mathcal{R}$ whose differences generate an ideal $\mathcal{I}_2 \lhd \mathcal{R}\surd$. In the quotient ring $\mathcal{R}\surd/\mathcal{I}_2$ these differences are 0.

For the basic facts about rings, ideals, reduced polynomials and Groebner basis we refer to [1].

(3.2) Lemma. *Let $\mathcal{I}_2 \lhd \mathcal{R}\surd$ be given by $\langle \mathcal{P}_2 \rangle$, where*

$$\mathcal{P}_2 = \left\{ z^2x^2+abxy-1,\ abx^2-1,\ zbx+ajy-0,\ ejx^2-1,\ zax+bey-0,\ abxy+ejy^2-1 \right\}.$$

Suppose T and T' are well-connected tangles differing by a restricted Reidemeister move 2. Then, $[T]+\mathcal{I}_2 = [T']+\mathcal{I}_2$, in $\mathcal{R}\surd/\mathcal{I}_2$.

3.2 Forcing invariance under Reidemeister move 3

The Reidemeister move 3 is entirely local for our evaluation. Therefore each one of the 18 pairs of fragments in Fig. 6 is indeed what it shows, a pair of $(0,0,1)$-tangles with a complete state assigned. Each term of a pair evaluates as a polynomial. The monomial factor ϕ_i takes care of the (common) boundary, which might have (globally) any pattern of coincidences among their faces. The point is that these patterns are the same in both sides and can be absorbed by the common factor ϕ_i. Let $\mathcal{I}_3$ be the ideal of $\mathcal{R}'$ generated by the difference of the polynomials of all the pairs after cancelling the common factors. We filter below, from Fig. 6, the 11/18 differences (in view of coincidences and disregarding boundaries 0,9,18,36 which are identically 0):

$$\begin{array}{rrrlrr}
1,2) & z^2x+bey-zbx & 4) & z^2bx+a^2jy-zb^2x & 5,20,40) & zbx+ejy-bjx \\
8) & zbx-z^2x-bey & 10) & b^2ex-za^2x-be^2y & 16) & z^2x+bey-zbx \\
17) & za^2x+be^2y-b^2ex & 21) & a^2bx+e^2jy-ej^2x & 32) & zb^2x-z^2bx-a^2jy \\
34) & abjx-zabx-aejy & 42) & ej^2x-a^2bx-e^2jy. & &
\end{array}$$

Denote by $\mathcal{P}_3$ the set of these eleven polynomials.

(3.3) Lemma. *Let $\mathcal{I}_3$ be the ideal $\langle \mathcal{P}_3 \rangle$. Suppose T and T' are well-connected tangles differing by a Reidemeister move 3. Then, the equality $[T]+\mathcal{I}_3 = [T']+\mathcal{I}_3$ holds in the quotient ring $\mathcal{R}\surd/\mathcal{I}_3$.*

Proof. All the possibilities for the states of the pair of $(0,0,1)$-tangles defined by move 3 are given in Fig. 6. Each member of $\mathcal{P}_3$ is 0 in the quotient ring. This is sufficient to imply invariance and the result follows. $\square$

4 An invariant of strong regular isotopy for tangles

Saying that two tangles are *strongly regularly isotopic* means that one is transformed into the other by Reidemeister moves of type 3 and of type 2 restricted. From what we have so far, it is an easy matter to produce such an invariant. Let $\mathcal{P} = \mathcal{P}_2 \cup \mathcal{P}_3$, and $\mathcal{I} = \langle \mathcal{P} \rangle$.

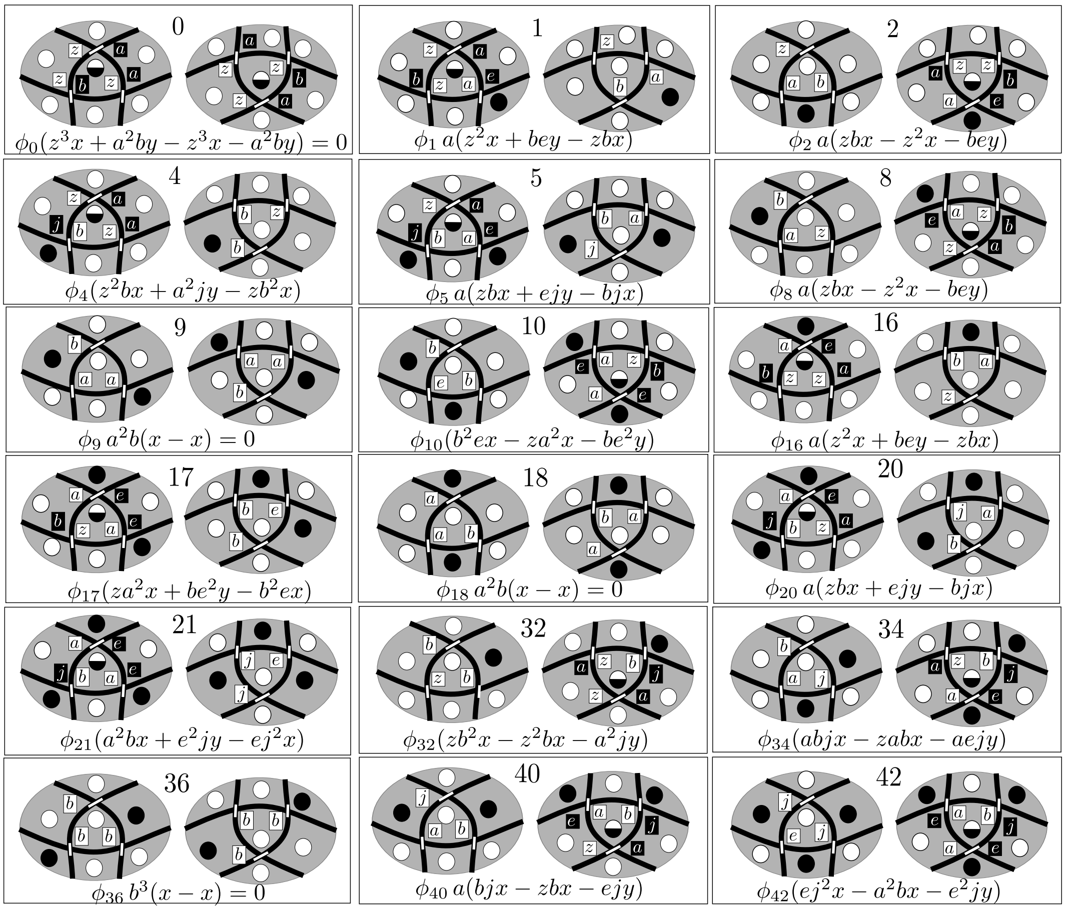

$\phi_0(z^3x + a^2by - z^3x - a^2by) = 0$ $\phi_1\, a(z^2x + bey - zbx)$ $\phi_2\, a(zbx - z^2x - bey)$

$\phi_4(z^2bx + a^2jy - zb^2x)$ $\phi_5\, a(zbx + ejy - bjx)$ $\phi_8\, a(zbx - z^2x - bey)$

$\phi_9\, a^2b(x - x) = 0$ $\phi_{10}(b^2ex - za^2x - be^2y)$ $\phi_{16}\, a(z^2x + bey - zbx)$

$\phi_{17}(za^2x + be^2y - b^2ex)$ $\phi_{18}\, a^2b(x - x) = 0$ $\phi_{20}\, a(zbx + ejy - bjx)$

$\phi_{21}(a^2bx + e^2jy - ej^2x)$ $\phi_{32}(zb^2x - z^2bx - a^2jy)$ $\phi_{34}(abjx - zabx - aejy)$

$\phi_{36}\, b^3(x - x) = 0$ $\phi_{40}\, a(bjx - zbx - ejy)$ $\phi_{42}(ej^2x - a^2bx - e^2jy)$

Figure 6: Eleven polynomials inducing invariance of tangle evaluation under Reidemeister move 3. Here the boundaries of the tangle pair defining the move coincide. Any identification pattern of faces in the boundary is allowed because the pattern is the same in both tangles. Thus their evaluation, possibly containing square roots, constitutes the factor ϕ_i common to both sides of a configuration of dots in the boundary.

Given a total order in the set of monomials of a polynomial ring, we can *reduce a polynomial relative to an ordered set of generators and a fixed monomial order for an ideal $\mathcal{I}$ of the ring.* This produces a well determined *reduced polynomial.* If the generating set is an ordered *Groebner basis* for $\mathcal{I}$, then the reduced polynomial is canonical, meaning that, if $p + \mathcal{I} = q + \mathcal{I}$ and p, q are reduced polynomials relative to an ordered Groebner basis and a given monomial order, then $p = q$ in the original ring $\mathcal{R}$. See a proof in [1]. For our purposes, this is the crucial property of Groebner bases.

Choose an arbitrary but fixed ordered Groebner basis $\mathcal{G}$ for $\mathcal{I} = \langle \mathcal{P} \rangle$, relative to a fix monomial order. As a matter fact this task takes only a few seconds in Singular [2] or Mathematica [9]. Denote by $[T]_\mathcal{G}$ the reduced form of the polynomial $[T]$ relative to $\mathcal{G}$.

(4.1) Theorem. *The mapping that associates $[T]_\mathcal{G}$ to a tangle T is an invariant of strong regular isotopy.*

Proof. Straightforward. □

5 Behavior of $[\ \ ]_\mathcal{G}$ under a curl creation/cancellation

(5.1) Lemma. *In the quotient ring $\mathcal{R}^{\surd}/\mathcal{I}$ the following equalities hold:*

$$hx + jy + \mathcal{I} = zx + by + \mathcal{I} = ex + \mathcal{I}, \qquad dx + ey + \mathcal{I} = zx + ay + \mathcal{I} = jx + \mathcal{I}.$$

Equivalently, we have $[hx + jy]_\mathcal{G} = [ex]_\mathcal{G} = [zx + by]_\mathcal{G}$ and $[dx + ey]_\mathcal{G} = [jx]_\mathcal{G} = [zx + ay]_\mathcal{G}$.

Proof. It follows from the analysis of Fig. 7: the curl passing through a crossing can be factored by moves 3 and 2 restricted. Therefore the two triples of $(0, 0, 1)$-tangles of the figure have the same evaluation. The common factor ϕ accounts for the boundary faces and the two crossings which need not to be specified. □

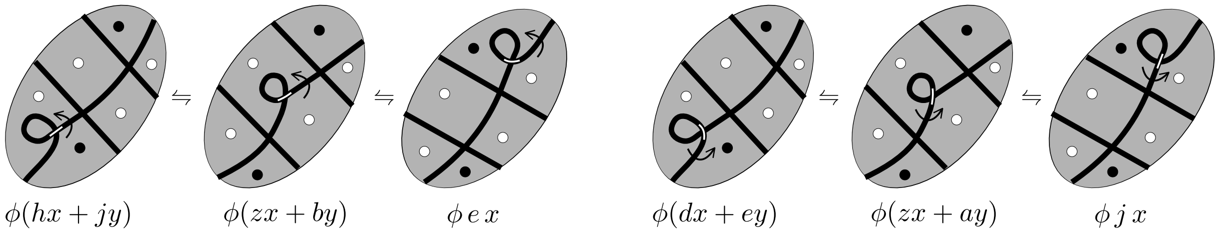

Figure 7: Curls passing through crossings

(5.2) Corollary. *(a) if T' is a tangle obtained from T by adding a positive curl, then $[T']_{\mathcal{G}} = (e\,x)_{\mathcal{G}}[T]_{\mathcal{G}}$. (b) if T' is a tangle obtained from T by adding a negative curl, then $[T']_{\mathcal{G}} = (j\,x)_{\mathcal{G}}[T]_{\mathcal{G}}$. (c) the equality $(e\,x)_{\mathcal{G}}\ (j\,x)_{\mathcal{G}} = 1$ holds in $\mathcal{R}\surd$.*

Proof. Parts (a) and (b) are direct consequence of Lemma 5.1. To prove part (c) let T be the $(0,1,1)$-tangle consisting of a single edge with their endpoints in the boundary and no crossings. Let T' be obtained from T by adding a pair of curls with opposite signs and rotation number. By Whitney's trick we have $[T']_{\mathcal{G}} = [T]_{\mathcal{G}}$. Together with previous parts (a) and (b) this implies that $(e\,x)_{\mathcal{G}}\ (j\,x)_{\mathcal{G}} = 1$, so . ☐

A *ribbon move in a tangle* (page 130 of [4]) is the replacement of a curl by another curl with the same sign and distinct rotation number.

(5.3) Corollary. *If T and T' are tangles differing by a ribbon move, then $[T']_{\mathcal{G}} = [T]_{\mathcal{G}}$.*

Proof. Straightforward from parts (a) and (b) of Corollary 5.2. ☐

Let $w(T)$ denote the total writhe, that is the algebraic sum of the signs of the crossings for an oriented form of a tangle T.

(5.4) Definition. (a) Given an oriented tangle T with $w(T) \geq 0$, let $\lceil T \rceil := (j\,x)^{w(T)}[T]$. (b) Given an oriented tangle T with $w(T) \leq 0$, let $\lceil T \rceil := (e\,x)^{-w(T)}[T]$.

(5.5) Theorem. *The mapping that associates $\lceil T \rceil_{\mathcal{G}}$ to an oriented tangle T is an invariant of strong regular isotopy and of Reidemeister move 1.*

Proof. Indeed, a strong move 2 or a move 3 do not change the value of $w(T)$ neither $[T]_{\mathcal{G}}$. As for move 1, addition of a positive curl, it multiplies $w(T)$ by $(j\,x)_{\mathcal{G}}$ and multiplies $[T]_{\mathcal{G}}$ by $(e\,x)_{\mathcal{G}}$. Thus, by part (c) of Corollary 5.2, $\lceil T' \rceil_{\mathcal{G}} = \lceil T \rceil_{\mathcal{G}}$. Anagously for the addition of a negative curl. ☐

6 Links on the sphere, long links on the plane

In this section we specialize S to be the 2-sphere or the plane. The tangle is then either a knot or a link or, in the case of S being the plane a long knot or a link with one infinite component, which we call a *long link* and which includes the long knot as a special case. In the pictures the sphere is presented as its northern hemisphere and the equator as a thick circle which is to be collapsed to a point. We let the diagram of a knot or link mean its $[\ \ ]_{\mathcal{G}}$-evaluation. If f is a face of T, we denote by $[T]^f_{\mathcal{G}}$ the $[\ \ ]_{\mathcal{G}}$-evaluation of T subject to the restriction that f always receives a black dot.

(6.1) Lemma. *Let T be a link on the sphere and f, g arbitrary faces. Then $[T]^f_{\mathcal{G}} = [T]^g_{\mathcal{G}}$, or pictorially, in the case of neighboring faces,*

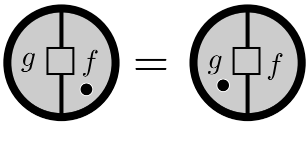

,

where inside the rectangle there is an arbitrary 1-1 tangle whose internal faces are unassigned.

Proof. It is enough to prove the lemma in the case that f and g share an edge. Consider the passages

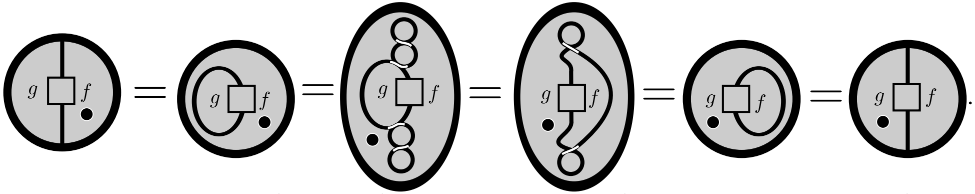

. The first is an isotopy; the second is the creation of a pair of 8's, by the inverse of two 8-moves; the third follows by regular isotopy; the fourth because the evaluation of opposite signed curls algebraically each other; the fifth is another isotopy. □

At this point is convenient to consider the following specialization of the $\{z, a, b, e, j, x, y\}$-variables:

(6.2) Definition. Let u be a primitive fifth root of the unity. Let the *u-assignment* be:

$$z \to -u^2 - u^3,\ a \to -u^3,\ b = h \to -u^2,\ e \to u^1,\ j \to u^4,\ x \to 1,\ y \to u^2 + u^3.$$

This assignment in principle can weaken the invariant, but so far, in practice, this did not occur. Let $[T]_u$ denote $[T]$ evaluated under the u-assignment.

(6.3) Lemma. *The* u-assignment *annihilate the 17 polynomials in $\mathcal{P}$, so* $[\ \ ]_u$ *is an invariant of strong regular isotopy.*

Proof. Routine verification. □

From now on we let u take the place of the Groebner basis $\mathcal{G}$. We note that Lemma 6.1 does not extend to surfaces of positive genus. Indeed, the black spot in each of the face assigned toroidal links below implies white spots throughout. Their u-evaluations are distinct contradicting Lemma 6.1,

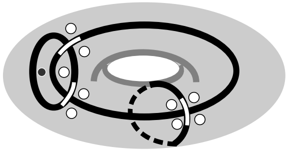
$= u + u^2 - u^4$

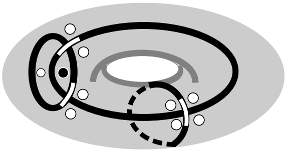
$= -u + u^3 + u^4$

.

Given a knot or a link on the sphere, removing a point in the interior of an edge produces a knot or link on the plane (represented in the pictures as a disk without the boundary). The knot becomes a long knot or a long link. There are two neighboring faces of of a long link that are unbounded. Our convention in the evaluation of a long link is that the spots on these infinite faces do not translate as $\sqrt{x}$ or $\sqrt{y}$, as if they were faces meeting the boundary. The diagrams for the long links are in open disks and do not include the boundary (which is at the infinite).

(6.4) Theorem. *Let T be a long knot or link on the plane and f and g faces sharing an edge. Then*

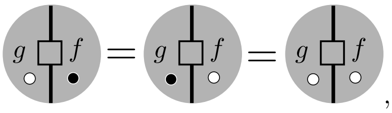

,

where inside the rectangle there is an arbitrary 1-1 tangle whose internal faces are unassigned.

Proof. The first equality follows from the Lemma 6.1 by dividing both members by $y = u^2 + u^3$. This is the same as multiplying by the inverse of y, which is $1 + y$. To prove the second equality we use 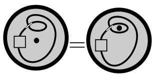 also justified by the same lemma. Thus,

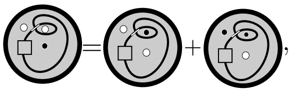
, or equivalently, cancelling the curl, e 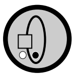 $= by$ 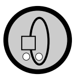 $+ jy$ 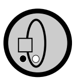 .

Opening to transform into long knots or links, noting that the first and third evaluations are equal by the Lemma 6.1 and dividing by y we have $e - j\,y$ 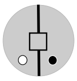 $= b$ 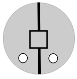. Finally, note that

$$e - jy = u - u^4(u^2 + u^3) = -u^2 = b.$$

Multiplying by $-u^3$ yields the second equality and the theorem. □

(6.5) Definition. If T is a long link on the plane and f, g are the infinite faces, define $\lfloor T \rfloor$ to be $\lceil T \rceil$ evaluated such the f and g always receive a white dot.

Theorem 6.4 has the following corollary:

(6.6) Corollary. $\lceil T \rceil_u =$ 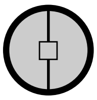 $= 1 + 2\,y$ 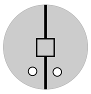 $= (1 + 2\,y)\,\lfloor T \rfloor_u$.

Proof. Straighforward. ☐

Note that we can invert: $y(1+y) = 1$ and $\frac{1}{5}(-u + u^2 + u^3 - u^4)(1 + 2y) = 1$. This last equality implies that for arbitrary links T on the sphere all the coefficients in $\lceil T \rceil_u$ are multiples of 5. Moreover, for the long forms we have multiplicativity under connected sums along the infinite strand:

(6.7) Theorem. *If T and T' are long links on the plane, then*

$$\lfloor T \,\#\, T' \rfloor_u = \lfloor T \rfloor_u \lfloor T' \rfloor_u.$$

Proof. The result follows directly from the definitions. ☐

Since there are long knots K satisfying $|\lfloor K \rfloor_u| > 1$ (See final Figs. 8 and 9) this theorem proves that the set

$$\mathcal{K}_u := \{\lfloor K \rfloor_u \mid K \text{ is a long knot in the plane}\},$$

is infinite. Indeed, there can be no bound for the absolute values of members of $\mathcal{K}_u$.

The expression for $\lfloor T \rfloor_u$ is normalized via $1 = -(u + u^2 + u^3 + u^4)$ to be put in the form $\lfloor T \rfloor_u = au + bu^2 + cu^3 + du^4 \equiv \lfloor a, b, c, d \rfloor_u$, where a, b, c, d are integers.

(6.8) Theorem. *Assume T and $T^\star$ mirror long links in the plane and $\lfloor T \rfloor_u = \lfloor a, b, c, d \rfloor_u$. Then, $\lfloor T^\star \rfloor_u = \lfloor d, c, b, a \rfloor_u$.*

Proof. It follows from the fact that $\lfloor T \rfloor_u$ and $\lfloor T^\star \rfloor_u$ are conjugate complex numbers. ☐

7 Appendix A: The values of the u-invariant for up to 10-crossings knots

We present in the next page $\lfloor K \rfloor_u$ for all for all prime knots K in $\mathbb{R}^3$ up to 10 crossing. Let $\mathcal{L}$ be the 52 upper and lower cases of the latin alphabet. The *contracted normal form* of the u-invariant is a *"4-letter word"* where each letter is taken from $\mathcal{L} \cup \{0, \alpha, \beta, \gamma\}$. To decode, take a,b,…z to mean respectively -1,-2,…,-26; take A,B,…Z to mean respectively 1,2,…,26; take 0 to mean 0, α to mean -27, β to mean -30 and γ to mean -33. Those 3 values are the only ones that have absolute value above 26. In this way each 4-code becomes a vector of 4 integers which are interpreted as the coefficients of u, u^2, u^3 and u^4 in $\lfloor K \rfloor_u$. Note that to obtain the invariant corresponding to the mirror knot it is enough to invert the 4-letter word. Therefore, knots which have distinct inverse pairs of 4-letter words like 8_{20} are not equivalent to their mirror image. We note that knot 8_{20} and the connected sum of a trefoil and its mirror image which are not distinguished by the Floer homology (according to [7]) are distinguished by the u-invariant.

7.1 Up to 7-crossings knots

3_1	0aAA	4_1	0bb0	5_1	ABBA	5_2	Aabb	6_1	abdb	6_2	BBab	6_3	beeb
7_1	AAa0	7_2	abdb	7_3	BECA	7_4	aded	7_5	DFEA	7_6	DBbc	7_7	chfb

7.2 8-crossings knots

8_1	Aabb	8_2	ACEB	8_3	beeb	8_4	DEB0	8_5	AEFD	8_6	eeaB	8_7	CCad
8_8	ehea	8_9	dhhd	8_{10}	EEac	8_{11}	DAed	8_{12}	ciic	8_{13}	dif0	8_{14}	Daff
8_{15}	FJFa	8_{16}	eaFF	8_{17}	elle	8_{18}	goog	8_{19}	aaaa	8_{20}	Aabb	8_{21}	Abec

7.3 9-crossings knots

9_1	aaaa	9_2	0bb0	9_3	baBB	9_4	DEB0	9_5	beeb	9_6	daCC	9_7	EFBb
9_8	EFBb	9_9	caEE	9_{10}	GIE0	9_{11}	BGIC	9_{12}	Bbhf	9_{13}	FICb	9_{14}	Aeif
9_{15}	Bdih	9_{16}	eaFF	9_{17}	dBGF	9_{18}	HJEb	9_{19}	bilf	9_{20}	DJLE	9_{21}	Dbig
9_{22}	cBIH	9_{23}	GJCd	9_{24}	fmlc	9_{25}	ileB	9_{26}	FCeh	9_{27}	dloh	9_{28}	geEH
9_{29}	ILCc	9_{30}	cmpg	9_{31}	HCfi	9_{32}	IFei	9_{33}	ispe	9_{34}	eqvj	9_{35}	dfgb
9_{36}	BIJE	9_{37}	ajme	9_{38}	JNFd	9_{39}	Demj	9_{40}	lfGL	9_{41}	ileB	9_{42}	ABBA
9_{43}	aBCB	9_{44}	cebA	9_{45}	ehea	9_{46}	ca00	9_{47}	DF0d	9_{48}	FBcd	9_{49}	AFIE

7.4 10-crossing knots

10_1	AAa0	10_2	bbaA	10_3	aded	10_4	BECA	10_5	AEFD	10_6	BGIC
10_7	Aeif	10_8	0BED	10_9	EEac	10_{10}	fhbB	10_{11}	GEbd	10_{12}	Cahh
10_{13}	0img	10_{14}	FNMC	10_{15}	0EIG	10_{16}	FFae	10_{17}	ciic	10_{18}	HFbf
10_{19}	bEJH	10_{20}	ehea	10_{21}	CJJC	10_{22}	ahlh	10_{23}	FBhi	10_{24}	imhA
10_{25}	HQPE	10_{26}	iplb	10_{27}	Fall	10_{28}	gibD	10_{29}	IGbh	10_{30}	Aipj
10_{31}	fome	10_{32}	jql0	10_{33}	fppf	10_{34}	eeaB	10_{35}	ahlh	10_{36}	ahlh
10_{37}	dmmd	10_{38}	ioia	10_{39}	FPNE	10_{40}	HAlk	10_{41}	JJah	10_{42}	htvi
10_{43}	hssh	10_{44}	LJbi	10_{45}	iwwi	10_{46}	cebA	10_{47}	AFIE	10_{48}	elle
10_{49}	eBJI	10_{50}	EMME	10_{51}	HBij	10_{52}	bFMI	10_{53}	LMBf	10_{54}	FJFa
10_{55}	IIaf	10_{56}	EPQH	10_{57}	Hamm	10_{58}	Aipj	10_{59}	LLag	10_{60}	mwpb
10_{61}	CE0b	10_{62}	AHJG	10_{63}	JIAd	10_{64}	HHad	10_{65}	F0ik	10_{66}	gCNK
10_{67}	akpk	10_{68}	Cbki	10_{69}	I0mo	10_{70}	gbIK	10_{71}	gttg	10_{72}	ITQE
10_{73}	IBlm	10_{74}	Chnj	10_{75}	nvoc	10_{76}	DMPH	10_{77}	Eblj	10_{78}	FQQF
10_{79}	fppf	10_{80}	fBML	10_{81}	iwwi	10_{82}	IIaf	10_{83}	mlBI	10_{84}	npbH
10_{85}	HMIA	10_{86}	mwpb	10_{87}	Altm	10_{88}	j$\alpha\alpha$j	10_{89}	LCmp	10_{90}	ktm0
10_{91}	hssh	10_{92}	KXWH	10_{93}	0IPK	10_{94}	JJah	10_{95}	KBmn	10_{96}	bqzn
10_{97}	aowo	10_{98}	HVUJ	10_{99}	jvvj	10_{100}	AJPI	10_{101}	MMai	10_{102}	alsl
10_{103}	HAlk	10_{104}	gttg	10_{105}	OMbj	10_{106}	LLag	10_{107}	jzxi	10_{108}	aINI
10_{109}	iwwi	10_{110}	MMai	10_{111}	HTTH	10_{112}	MMai	10_{113}	Kbtr	10_{114}	0pxn
10_{115}	l$\beta\beta$l	10_{116}	NNak	10_{117}	qqaK	10_{118}	kzzk	10_{119}	oαq0	10_{120}	QRBk
10_{121}	rqBN	10_{122}	qαpA	10_{123}	n$\gamma\gamma$n	10_{124}	ABBA	10_{125}	ABBA	10_{126}	cebA
10_{127}	EIFA	10_{128}	Aabb	10_{129}	ehea	10_{130}	BBab	10_{131}	bhie	10_{132}	ABBA
10_{133}	beeb	10_{134}	DBbc	10_{135}	bilf	10_{136}	ACEB	10_{137}	Baee	10_{138}	bCIF
10_{139}	0CC0	10_{140}	0B0a	10_{141}	ccaC	10_{142}	CAba	10_{143}	dhcA	10_{144}	hf0E
10_{145}	CBA0	10_{146}	afkf	10_{147}	EHC0	10_{148}	fieA	10_{149}	HMIA	10_{150}	EIFA
10_{151}	HFbf	10_{152}	aaaa	10_{153}	BBab	10_{154}	cebA	10_{155}	Baee	10_{156}	eaFF
10_{157}	IPJA	10_{158}	fome	10_{159}	glfA	10_{160}	aCFC	10_{161}	Aabb	10_{162}	EBef
10_{163}	IGbh	10_{164}	gojb	10_{165}	dklg						

8 Appendix B: Image of the u-invariant of knots up to 10 crossings

We plot the complex numbers $\lfloor K \rfloor_u$ and their conjugates for all prime knots K up to 10 crossings evaluated at $u = e^{\frac{2\pi i}{5}}$ and $u = e^{\frac{4\pi i}{5}}$. Since all mirror pairs of knots are included, the graphic is symmetric relative to the real axis. Moreover we make these valued closed for all writhes of knots involved by multiplying each individual value obtained by $1, u, u^2, u^3$, and by u^4, including all 5 products in our data to be plotted. A dihedral 10-fold symmetry is then inherently present in the image. However, if we forget primality the image is much more dense: by Theorem 6.7 we could close it under multiplication.

In Fig. 8 we plot the image computed at $u = e^{\frac{2\pi i}{5}}$ and In Fig. 9 at $u = e^{\frac{4\pi i}{5}}$. The curious fact is the unexpected great difference in scale corresponding to the two values of u. Because of conjugacy of the complex numbers involved, note that the image corresponding to $u = e^{\frac{6\pi i}{5}}$ coincides with the one of $u = e^{\frac{4\pi i}{5}}$. The same is true for $u = e^{\frac{8\pi i}{5}}$ and $u = e^{\frac{2\pi i}{5}}$.

References

[1] D. Cox and J. Little. *Ideals, varieties & algorithms: An introduction to computational Algebraic Geometry & Commutative Algebra (Undergraduate Texts in Mathematics)*. Springer-Verlag, 2 edition, 2005.

[2] G.M. Greuel, G. Pfister, and H. Schönemann. Singular – a computer algebra system for polynomial computations. In *Symbolic computation and automated reasoning*, pages 227–233. AK Peters, Ltd., 2001.

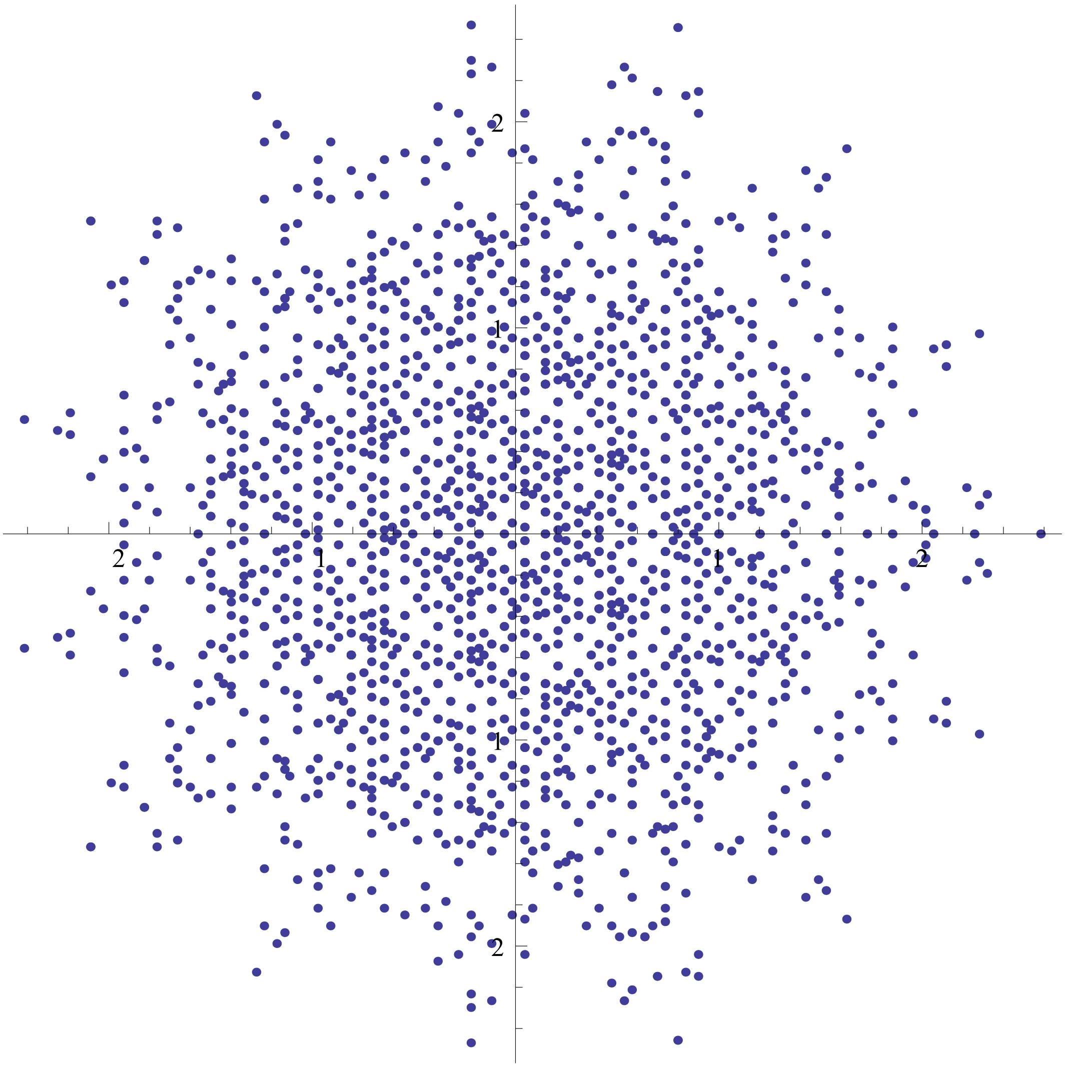

Figure 8: **The image of the u-invariant of knots up to 10 crossings computed at $u = e^{\frac{2\pi i}{5}}$**

[3] P. Johnson and S. Lins. A graphical calculus for tangles on surfaces. *arXiv:1210.6681v1 [math. GT]*, 2012.

[4] L.H. Kauffman and S. Lins. Temperley-Lieb Recoupling Theory and Invariants of 3-manifolds. *Annals of Mathematical Studies, Princeton University Press*, 134:1–296, 1994.

[5] WBR Lickorish. Three-manifolds and the Temperley-Lieb algebra. *Mathematische Annalen*, 290(1):657–670, 1991.

[6] N. Reshetikhin and V.G. Turaev. Invariants of 3-manifolds via link polynomials and quantum groups. *Inventiones mathematicae*, 103(1):547–597, 1991.

[7] T. Tanaka. Symmetric unions indistinguishable by knot Floer and Khovanov homology. pages 1–24. A talk in the Joint Meeting of Korean and American Math. Society, 2009.

[8] V.G. Turaev and O.Y. Viro. State sum invariants of 3-manifolds and quantum 6j-symbols. *Topology*, 31(4):865–902, 1992.

[9] S. Wolfram. Mathematica. Wolfram Research, version 8. *Symbolic Manipulation Software*, 2012.

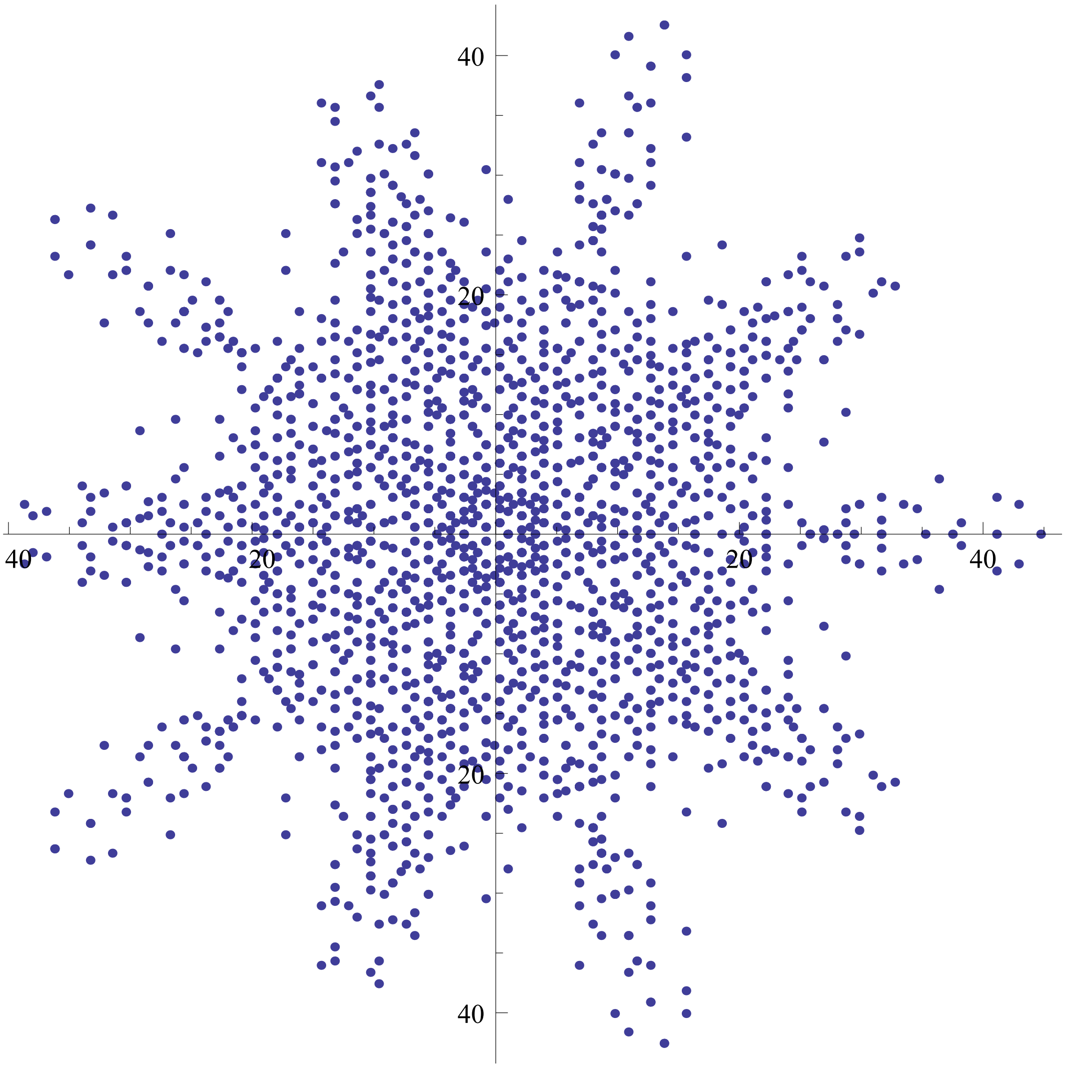

Figure 9: **The image of the u-invariant of knots up to 10 crossings computed at $u = e^{\frac{4\pi i}{5}}$**

Peter M. Johnson
Departamento de Matemática, UFPE
Recife–PE
Brazil
peterj@dmat.ufpe.br

Sóstenes Lins
Centro de Informática, UFPE
Recife–PE
Brazil
sostenes@cin.ufpe.br